MODELLING OF UAVS HOVERING IN EXTREME TEMPERATURE ENVIRONMENTS

An Undergraduate Research Scholars Thesis

by

DANIEL GONÇALVES GHAN

Submitted to the Undergraduate Research Scholars program at
Texas A&M University
in partial fulfillment of the requirements for the designation as an

UNDERGRADUATE RESEARCH SCHOLAR

Approved by Research Advisor: Dr. James Boyd

May 2017

Major: Aerospace Engineering

TABLE OF CONTENTS

ABSTRACT

Modelling of UAVs Hovering in Extreme Temperature Environments

Daniel Ghan
Department of Aerospace Engineering
Texas A&M University

Research Advisor: Dr. James Boyd
Department of Aerospace Engineering
Texas A&M University

As unmanned aerial vehicles (UAVs) become more widely available, they are being applied to an ever-widening range of tasks, especially in areas that are inaccessible or dangerous to humans. Of particular interest is the potential to use UAVs in extremely hot environments. Batteries and motors are sensitive to high temperatures, so UAVs operating in such an environment must be specially designed to resist the heat to survive as long as possible. To facilitate the design of UAVs for extreme temperature, we have developed a temperature-dependent mathematical model of a UAV. The motors and battery are modelled as separate entities surrounded by insulation, which greatly reduces heat transfer the outside the UAV, and phase-change material (PCM), which absorbs waste heat from the internal components. No other electrical components are modelled. Given the physical properties of various components, the model can predict the temperature of the internal components over time and the point at which the UAV is no longer capable of hovering. Preliminary results from a MATLAB simulation suggest that a commercial UAV with PCM and insulation could last several minutes in extreme heat.

ACKNOWLEDGEMENTS

I would like to thank Dr. Boyd for sponsoring this project, guiding my research for the past year and a half, and reviewing my writing. I would like to acknowledge the several students worked on this project before I did and compiled many of the equations. Unfortunately, I do not know most of their names; otherwise I would list them here. Finally, the Undergraduate Research Scholars program has supported the publication of my research.

LIST OF SYMBOLS

n	Number of motors on UAV

Masses:

m_m	Mass of each motor
m_b	Mass of the battery
m_{PCM_m}	Mass of phase-change material around each motor
m_{PCM_b}	Mass of phase-change material around battery
m_{ins_m}	Mass of insulation around each motor
m_{ins_b}	Mass of insulation around battery
$m_{payload}$	Mass of the mission payload
m_{other}	Mass of everything on the UAV not mentioned above (frame, wires, etc.)
m	Total mass of UAV

Environmental constants:

g	Acceleration due to gravity
p_∞	Air pressure
ρ_∞	Air density
R	Specific gas constant
T_∞	Air temperature

Thermodynamics:

U_m	Energy of the motor
U_b	Energy of the battery
Q_m	Rate of heat transfer into the motor
Q_b	Rate of heat transfer into the battery
W_m	Net work done by the motor
W_b	Net work done by the battery

Heat transfer:

T_m	Temperature of the motors
T_b	Temperature of the battery
T_{PCM_m}	Temperature of the motor PCM
T_{PCM_b}	Temperature of the battery PCM
R_{c_m}	Thermal resistance between motor and motor PCM
R_{T_m}	Thermal resistance between motor and environment
$R_{T_{PCM_m}}$	Thermal resistance between motor PCM and environment
R_{c_b}	Thermal resistance between battery and battery PCM
R_{T_b}	Thermal resistance between battery and environment
$R_{T_{PCM_b}}$	Thermal resistance between battery PCM and environment

Motor and propeller properties:

C_F	Thrust coefficient
C_T	Torque coefficient
c_m	Specific heat capacity of the motors
I_m	Current drawn by each motor
V_m	Potential drawn by the motors
F	Thrust from each propeller
K_V	Voltage constant
M_m	Motor torque
M_L	Load torque
M_{frict}	Frictionally-generated torque
ρ_m	Resistivity of the armature
R_m	Resistance of the armature
r	Radius of the propellers
η	Motor efficiency
Ω	Angular velocity of the propellers

Battery properties:

α	Current-dependent coefficient for state of discharge
β	Temperature-dependent coefficient for state of discharge
c_k	k^{th}-order coefficient of polynomial approximation of discharge curve
c_b	Specific heat capacity
I_b	Current drawn from the battery
E_b	Potential between the terminals
V_b	Open-circuit potential
C	Nominal battery capacity
R_b	Internal resistance of the battery
SOD	State of discharge

Phase-change material properties:

L	Specific latent heat capacity
ρ_{PCM}	Density
c_{PCM}	Specific heat capacity

SECTION I

INTRODUCTION

As unmanned aerial vehicles (UAVs) become more widely available, they are being applied to an ever-widening range of tasks, especially in areas that are inaccessible or dangerous to humans. Of particular interest is the potential to use UAVs in extremely hot environments; for example, to search for victims in a burning building, or fly into the heart of an inferno to seal off a fuel line. Because the batteries and motors in most UAVs are sensitive to high temperatures, one operating in such an environment must be specially designed to resist the heat to survive as long as possible.

To aid in this task, Dr. James Boyd and I have developed a model to predict a UAV's survival time in extreme heat. The motors and battery are modelled as separate entities surrounded by insulation, which greatly reduces heat transfer the outside the UAV, and phase-change material (PCM), which absorbs waste heat from the internal components. No other electrical components are modelled. Using equations describing heat transfer and the performance of the motors, propellers, and battery, the model can predict the temperature of the internal components over time and the point at which the UAV is no longer capable of hovering.

SECTION II

MODEL

A. Model Equations

A typical UAV consists of a frame, a battery, electronics, several motors and propellers, and a payload. To function for a reasonable length of time, a UAV in an extremely hot environment would also need insulation and phase-change material (PCM) around the battery and motors. The insulation is required to prevent heat transfer from the outside environment, and the PCM is needed to absorb waste heat from the components (which obviously cannot be vented to the outside). In this model, all electronic components other than the battery and motors are ignored, except for the implied existence of electronic speed controllers (ESCs) to regulate the input voltage for the motors.

This model takes into account the effects of heat transfer on the battery and motors. Each of these components is assumed to be separated and encased in PCM and insulation, as shown in Figure 1.

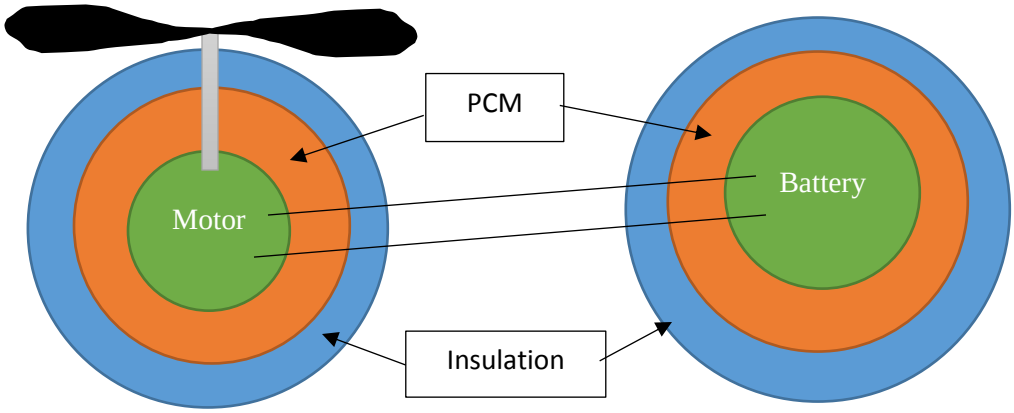

Figure 1

The total mass of the UAV is the sum of the masses of the components:

$$m = m_b + m_{PCM_b} + m_{ins_b} + n(m_m + m_{PCM_m} + m_{ins_m}) + m_{other} + m_{payload} \quad (1)$$

where m is the total mass; n is the number of motors; m_b is the mass of the battery; m_m is the mass of each motor; m_{PCM_m} and m_{PCM_b} are the masses of the PCM surrounding each motor and the battery, respectively; m_{ins_m} and m_{ins_b} are the masses of the insulation surrounding each motor and the battery, respectively; $m_{payload}$ is the mass of the payload, which is treated as a mission parameter; and m_{other} is the mass of everything else, including the frame, electronics, and propellers.

Typically, the motors on a UAV are connected in parallel. Because all the other electronics are neglected, the current from the battery is the sum of the currents through all the motors:

$$I_b = nI_m \quad (2)$$

And each motor can receive the full potential difference of the battery.

The model determines whether the UAV can remain hovering by calculating, separately, the supply voltage required by the motors and the voltage across the battery terminals. If the battery voltage is greater, the excess can be dissipated by the ESCs. Thus the **condition for failure** is

$$E_b < V_m \tag{3}$$

where E_b is the voltage across the battery terminals and V_m is the motors' required supply voltage.

1. Flight Dynamics

The model assumes that the UAV is hovering in one place; by Newton's Second Law, this means that the sum of the forces acting on it is zero. The two forces acting on a hovering UAV are gravity and lift; therefore

$$nF = mg \tag{4}$$

where F is the force generated by each propeller. This force can also equal to

$$F = \frac{\pi}{2}\rho_\infty \Omega^2 r^4 C_F \tag{5}$$

where ρ_∞ is the density of the air, Ω is the angular velocity, r is the radius of the propeller, and C_F is a constant that can be determined experimentally [1]. Similarly, the torque generated by aerodynamic drag can be written as

$$M_L = \frac{\pi}{2}\rho_\infty \Omega^2 r^5 C_T \tag{6}$$

where C_T is another experimentally-determined constant.

According to the ideal gas law,

$$p_\infty = \rho_\infty R T_\infty \tag{7}$$

where p_∞ is pressure, R is a specific gas constant, and T_∞ is temperature. Substituting Equations (4) and (7) into (5), we find that the angular momentum of the propellers is

$$\Omega = \sqrt{\frac{2mgT_\infty R}{np_\infty \pi r^4 C_F}} \tag{8}$$

By dividing Equation (6) by Equation (5) and substituting Equation (4), the load torque can be written as

$$M_L = \frac{mgrC_T}{nC_F} \tag{9}$$

2. Motor Model

At steady state, the angular velocity of the motors is

$$\Omega = \frac{V_m - I_m R_m}{K_V} \tag{10}$$

where V_m is the supply voltage, K_V is a voltage constant, I_m is the current, and R_m is the resistance of the armature. The torque output by the motor is

$$M_m = K_T I_m = K_V I_m \tag{11}$$

where K_T is the torque constant. If written in equivalent units (e.g. $\frac{V \cdot s}{rad}$ and $\frac{N \cdot m}{A}$), K_T is equivalent to K_V [2]. The output torque is assumed to be comprised of two components:

$$M_m = M_L + M_{frict} \tag{12}$$

where M_L is the load torque and M_{frict} is associated with friction in the motor.

The electrical power put into the motor is

$$V_m I_m = K_V \Omega I_m + I_m^2 R_m \tag{13}$$

If M_{frict} is neglected (i.e. $M = M_L$), the mechanical power output is

$$M_L \Omega = K_V I_m \Omega \tag{14}$$

and the loss (which becomes waste heat) is

$$V_m I_m - M_L \Omega = I_m^2 R_m \tag{15}$$

Due to demagnetization, the voltage constant of a motor decreases linearly with temperature:

$$K_V = K_{V_i}\left(1 + \alpha_{mag}\left(T_m - T_{ref}\right)\right) \tag{16}$$

where K_{V_i} is the voltage constant provided by the manufacturer, α_{mag} is a negative temperature coefficient, and T_{ref} is a reference temperature [2].

R_m is assumed to increase linearly with temperature:

$$R_m = R_{m_i}\left(1 + \alpha_R\left(T_m - T_{ref}\right)\right) \tag{17}$$

where R_{m_i} is a reference resistance, α_R is a temperature coefficient, and T_{ref} is another reference temperature. If the armature is a wire of uniform composition and cross-sectional area, the resistance can be calculated:

$$R_{m_i} = \frac{\rho_{m_i} l}{A} \tag{18}$$

where ρ_{m_i} is the resistivity of the armature, l is its length, and A is its cross-sectional area.

3. Battery Model

Using the notation of [3], the state of discharge of the battery is defined by

$$SOD(t) = \frac{1}{C}\int_0^t \alpha\beta I_b \, d\tau \tag{19}$$

where α is a function of current, β is a function of temperature, and C is the nominal capacity. α and β must be determined experimentally.

The open-circuit voltage of the battery is given by

$$V_b = \sum_{k=0}^{n} c_k SOD^k + \Delta E \tag{20}$$

where the summation represents an n^{th}-order polynomial approximation of the discharge curve and ΔE is an experimentally-determined temperature-dependent function. The output voltage (that available to the motors and other components) is

$$E_b = V_b - I_b R_b \tag{21}$$

where R_b is the internal resistance of the battery. The resistance is assumed to be constant with respect to temperature, but the experimental design introduced by [3] allows changes in resistance to be reflected in the term ΔE.

4. Heat Transfer

According to the first law of thermodynamics,

$$\dot{U} = \dot{Q} - \dot{W} \tag{22}$$

where U is the internal energy of a system, Q is the heat transferred into the system, and W is the work done by the system on its surroundings. This equation can be applied to the battery and each motor separately to calculate the temperature change in each component.

Heat transfer between any two surfaces is assumed to proportional to the different in their temperatures. The constants of proportionality must be determined by experiment or estimated by calculations such as those shown in Appendix 2.

Motors

Motors are devices that convert electrical work into mechanical work. Therefore, the net work rate done by the motor is the electrical power input subtracted from the mechanical power output:

$$\dot{W}_m = M_L\Omega - I_m V_m \tag{23}$$

Or, substituting Equation (15),

$$\dot{W}_m = -I_m^2 R_m \tag{24}$$

Because there are no chemical changes or changes in kinetic or potential energy in the motor, we can say that

$$\dot{U}_m = m_m c_m \dot{T}_m \tag{25}$$

where m_m is the mass of the motor, c_m is its specific heat capacity, and T_m is its average temperature.

The heat transfer to the motor can be written as

$$\dot{Q}_m = \frac{T_\infty - T_m}{R_{T_m}} + \frac{T_{PCM_m} - T_m}{R_{c_m}} \tag{26}$$

where T_{PCM_m} is the temperature of the PCM surrounding the motor, R_{T_m} is the thermal resistance between the motor and the outside environment, and R_{c_m} is the thermal resistance between the motor and the surrounding PCM.

Substituting Equations (24) through (26), Equation (22) can be written as

$$m_m c_m \dot{T}_m = I_m^2 R_m + \frac{T_\infty - T_m}{R_{T_m}} + \frac{T_{PCM_m} - T_m}{R_{c_m}} \tag{27}$$

Battery

The battery is a device that converts chemical energy into electrical work. The work done by the battery is

$$\dot{W}_b = I_b E_b \tag{28}$$

The battery has constant kinetic and potential energy, but its internal energy changes due to both chemical reactions and temperature change:

$$\dot{U}_b = m_b c_b \dot{T}_b - I_b V_b \tag{29}$$

The heat transfer to the battery can be written as

$$\dot{Q}_b = \frac{T_\infty - T_b}{R_{T_b}} + \frac{T_{PCM_b} - T_b}{R_{c_b}} \tag{30}$$

where T_{PCM_b} is the temperature of the PCM surrounding the battery, R_{T_b} is the thermal resistance between the battery and the outside environment, and R_{c_b} is the thermal resistance between the battery and the surrounding PCM.

Substituting Equations (28) through (30) and (21), Equation (22) can be written as

$$m_b c_b \dot{T}_b = I_b^2 R_b + \frac{T_\infty - T_b}{R_{T_b}} + \frac{T_{PCM_b} - T_b}{R_{c_b}} \tag{31}$$

Phase-Change Material

The phase-change material does not do any work. Before and after the phase change, its energy is dependent only on its temperature:

$$\dot{U} = m_{PCM} c_{PCM} \dot{T}_{PCM} \tag{32}$$

Heat transfer to the PCM surrounding the motor is given by

$$\dot{Q}_{PCM_m} = \frac{T_{PCM_m} - T_m}{R_{c_m}} + \frac{T_{PCM_m} - T_\infty}{R_{T_{PCM_m}}} \tag{33}$$

Substituting Equations (32) and (33) into Equation (22) yields

$$m_{PCM} c_{PCM} \dot{T}_{PCM_m} = \frac{T_\infty - T_{PCM_m}}{R_{T_{PCM_m}}} + \frac{T_m - T_{PCM_m}}{R_{c_m}} \tag{34}$$

Similarly, for the battery's PCM,

$$m_{PCM}c_{PCM}\dot{T}_{PCM_b} = \frac{T_\infty - T_{PCM_b}}{R_{T_{PCM_b}}} + \frac{T_b - T_{PCM_b}}{R_{c_b}} \quad (35)$$

During the phase change, the temperature of the PCM remains constant; the internal energy is increased by breaking intermolecular bonds. Each unit mass of PCM can absorb a certain amount of energy this way, defined by the latent heat capacity of the material, L.

B. Model Input Parameters

1. Summary

Table 1Table 1 lists the general UAV properties and parameters that would vary for each mission (in which case the values given reflect the range used to build the graphs in Section III).

through Table 5 list the model's inputs. Knowing these parameters is necessary and sufficient for determining how long a UAV can continue to hover.

To demonstrate the model, I programmed it into MATLAB using a simple Euler algorithm for integration. I estimated values for each input parameter based on the DJI Matrice 100, a quadcopter that uses DJI E800 3510 motors and, for my purposes, a DJI TB48D battery. These values are listed next to each parameter in the tables, and the following subsections explain the basis for any estimations not taken directly from DJI's documentation.

Mission Parameters and Initial Conditions

Table 1 lists the general UAV properties and parameters that would vary for each mission (in which case the values given reflect the range used to build the graphs in Section III).

Table 1

Quantity	Symbol	Value	Comments and References
Total mass of UAV	m	3071g	Equation (1); includes 1331g frame, 300g payload, and 230g of insulation.
Atmospheric Temperature	T_∞	300°C	
Atmospheric Pressure	p_∞	101325 Pa	Standard atmospheric pressure at sea level
Gravity	g	9.807 m/s^2	Standard Earth gravity
Specific gas constant	R	287.04 J/kg·K	Standard specific gas constant for air
Number of motors	n	4	[4]
Mass of PCM around each motor	m_{PCM_m}	10.6g	10% of motor mass
Mass of PCM around battery	m_{PCM_b}	67.6g	10% of battery mass
Initial temperature of motors and motor PCM		–40°C	The motors are significantly more efficient at lower temperatures.
Initial temperature of battery and battery PCM		0°C	The battery's life can be significantly extended by cooling it before flight.
Initial state of discharge		0	Battery starts fully charged

Propellers

Table 2 lists the properties of the propellers.

Table 2

Quantity	Symbol	Value	Comments and References
Propeller torque constant	C_T	0.0035	
Propeller thrust constant	C_F	0.034	
Radius of propellers	r	173mm	[4], pages 65 and 66

Motor

Table 3 lists the properties of the motors.

Table 3

Quantity	Symbol	Value	Comments and References
Reference voltage constant	K_{V_i}	0.0273 V·s/rad	[5]; reference temperature is 25°C
Magnetic temperature coefficient	α_{mag}	-0.0012 K^{-1}	[2]
Mass of each motor	m_m	106g	[5]
Specific heat capacity	c_m	386 J/kg·K	
Reference resistance of armature	R_{m_i}	0.8182Ω	Reference temperature is 20°C
Resistance temperature coefficient	α_R	0.00386 K^{-1}	
Frictional torque	M_{frict}	0	Frictional torque is neglected in the simulations.

Batteries

Table 4 lists the properties of the battery.

Table 4

Quantity	Symbol	Value	Comments and References
Mass	m_b	676g	[4], page 61
Internal resistance	R_b	168mΩ	
Nominal Capacity	Q_r	20520C	[4], page 61
Current coefficient	α	Function of current	
Temperature coefficient	β	Function of temperature	
Polynomial coefficients of potential	c_k		4 terms (cubic function)
Temperature contribution to potential	ΔE	Function of temperature	
Specific heat capacity	c_b	1040 J/kg·K	[6]

Phase-Change Material

PCM S46 was chosen as the phase-change material. Table 5 lists its properties.

Table 5

Quantity	Symbol	Value	Comments and References
Temperature of phase change	T_{trans}	46°C	[7]
Specific heat	c_{PCM}	2410 J/kg·K	
Specific latent heat of transformation	L	210 kJ/kg	

Thermal Resistances

Table 6 lists the thermal resistances calculated in Appendix 2.

Table 6

Surfaces	Symbol	Value
Motor and motor PCM	R_{c_m}	1.28 K/W
Motor and environment	R_{T_m}	29.1 K/W
Motor PCM and environment	$R_{T_{PCM_m}}$	141 K/W
Battery and battery PCM	R_{c_b}	0.00807 K/W
Battery and environment	R_{T_b}	∞
Battery PCM and environment	$R_{T_{PCM_b}}$	12.5 K/W

2. Propellers

The required current and voltage in the motor are directly related to the propeller's radius; thrust constant, C_F; and torque constant, C_T. Of these parameters, only the radius (173mm) is readily available for the Matrice 100's DJI 1345s propellers.

Figure 2 shows values of C_F and C_T for many different propellers at 6000rpm from the University of Illinois's Propeller Data Site [1].

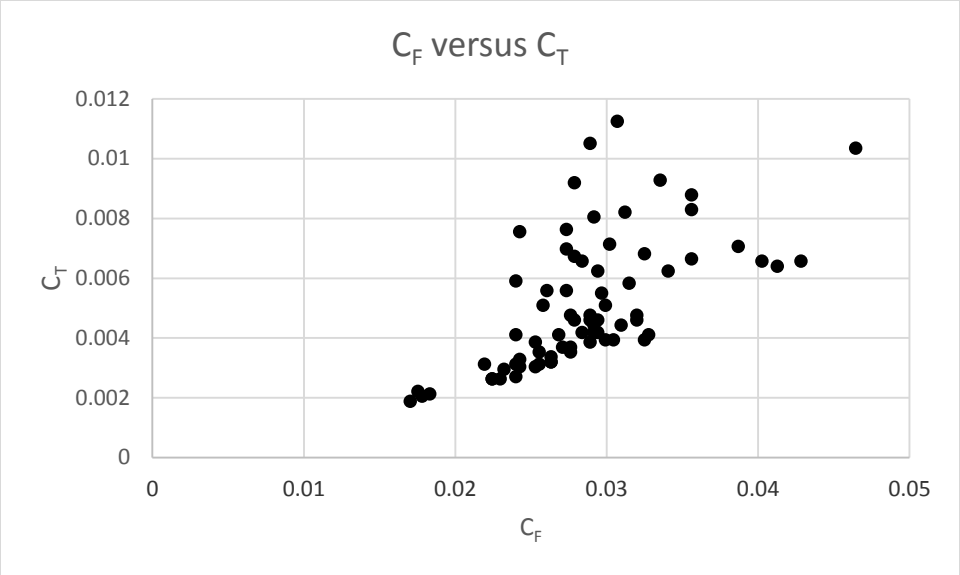

Figure 2

In order for the UAV to be able to hover under the most extreme conditions simulated (500, C_F must be at least about 0.034. Based on Figure 2, the lowest C_T that seems reasonable for a C_F of 0.034 is about 0.0035.

3. Motors

The simulated motor is based on the DJI 3510, the motor that comes with the Matrice 100. This motor has a nominal voltage constant of 350 rpm/V and a mass of 106g [5].

Voltage Constant

The magnets in the motors are assumed to be made of Neodymium Iron Boron, a common material in high-end DC motors, which has a magnetic temperature coefficient of –0.0012 and a reference temperature of 25°C [2].

Resistance

The armature is probably made of copper, whose resistivity has a temperature coefficient of 0.00386 K^{-1}. The reference resistance was calculated by assuming that the DJI 3510, a high-end, DC brushless motor, would have an efficiency of around 85% when operating under normal conditions.

The motor's efficiency factor is defined as

$$\eta \equiv \frac{P_{out}}{P_{in}} = \frac{\Omega M_L}{I_m V_m} \tag{36}$$

where P_{out} is the mechanical energy output by the motor (torque × angular rate) and P_{in} is the electrical energy put into the motor (current × potential). If friction is neglected, Equations (14) and (10) can be substituted to simplify the expression to

$$\eta = 1 - \frac{I_m R_m}{V_m} \tag{37}$$

The Matrice 100, with the TB48D battery and no payload, discharges 90% in 28 minutes [4]. Because the TB48D's capacity is 20520C, the current must be 11.0A—2.75A per motor. Assuming the Matrice 100 could hover until its battery was fully discharged, its motors probably require 15V (the minimum voltage of lithium-polymer batteries is generally considered to be 2.5V per cell [3]). Substituting these values into Equation (37) produces a resistance of 0.8182Ω.

Specific Heat Capacity

The specific heat of the motor is assumed to be that of copper, which makes up a significant portion of the motors' mass: 386 J/kg·K.

4. Battery

The simulated battery is based on the DJI TB48D, the larger of the two batteries sold for the Matrice 100. The TB48D is a 6-cell lithium-polymer battery that is 676g and has a nominal capacity of 20520C [4].

Internal Resistance

[8] describes measurements of internal resistance, among other things, in 7920C lithium-ion cells often used in RC aircraft. The median internal resistance was 28mΩ; multiplying by 6 cells in series brings the total resistance to 168mΩ for a battery like the TB48D.

State of Discharge

As seen in Equation (19), the battery's state of discharge depends on a current-dependent factor, α, and a temperature-dependent factor, β.

α was approximated as a linear function based on data from [3], adjusted for the greater capacity of the TB48D. It is shown in Figure 3.

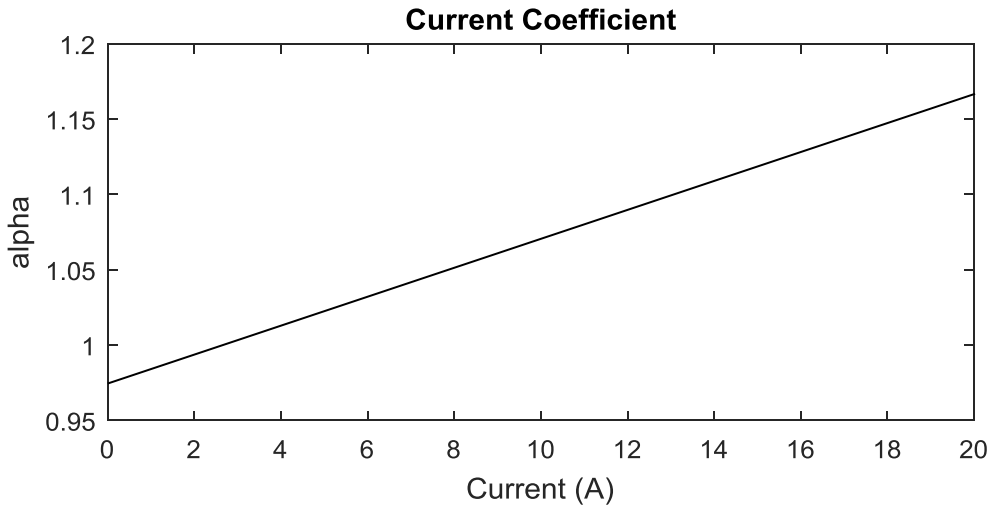

Figure 3

Similarly, β was approximated by a linear function based on data from [3]. It is shown in Figure 4.

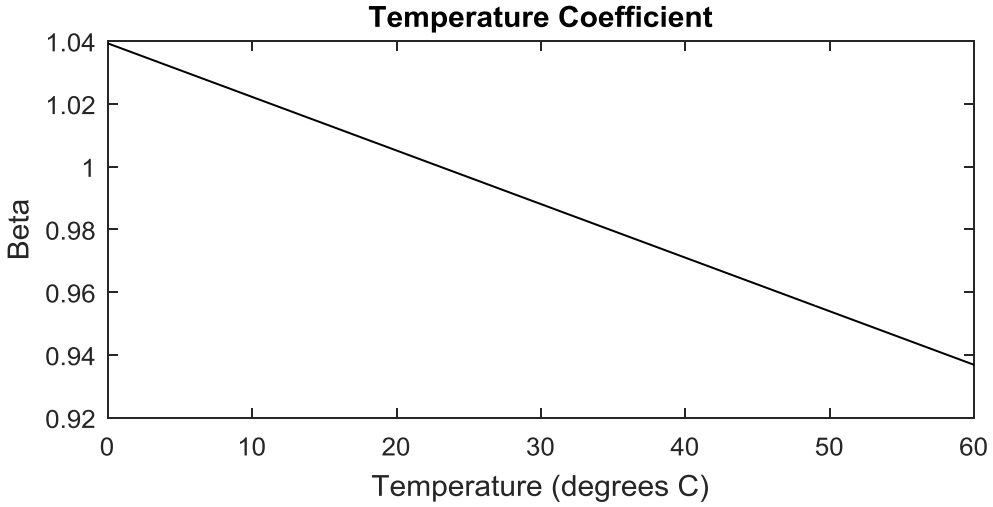

Figure 4

Battery Potential

As per Equation (20), the battery's open-circuit potential is a function of its state of discharge, known as a discharge curve, plus a function of temperature.

The discharge curve was approximated by a fitting a cubic polynomial to data from [3] using the least-squares method. The data and the polynomial approximation of the discharge curve are shown in Figure 5.

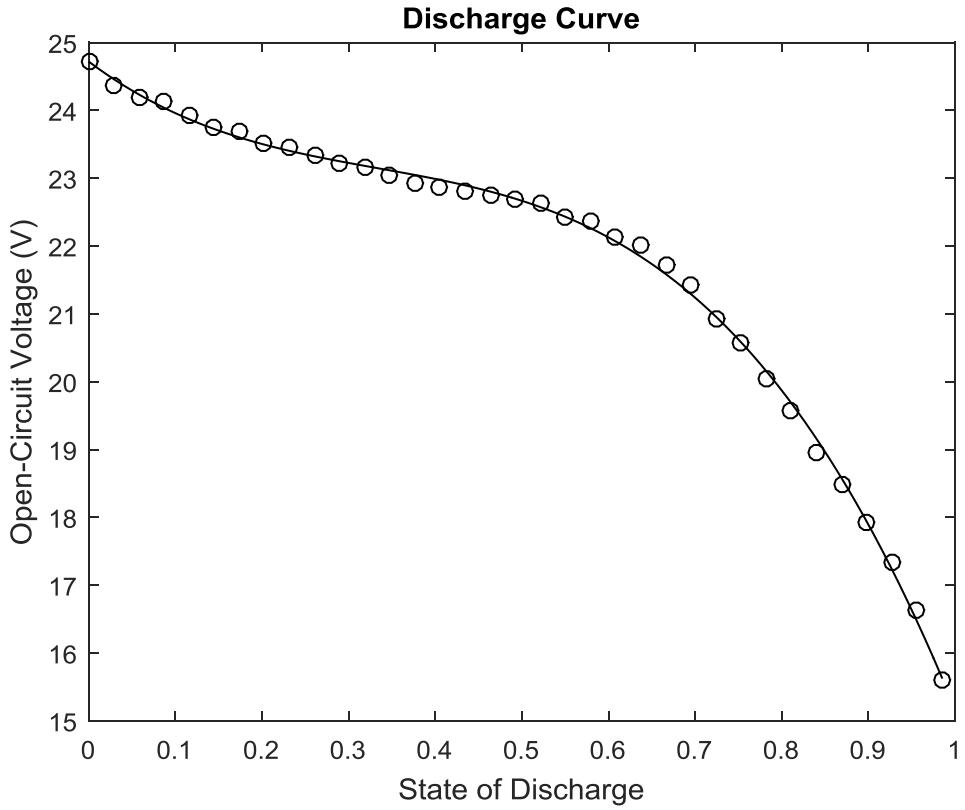

Figure 5

The temperature-dependent function was approximated by fitting a 5^{th}-order polynomial to a combination of data from [3], which ranged from -20°C to 45°C and estimated data points

designed to capture the battery's sudden decrease in performance around 60°C. The "data" points and the approximation for this function are shown in Figure 6.

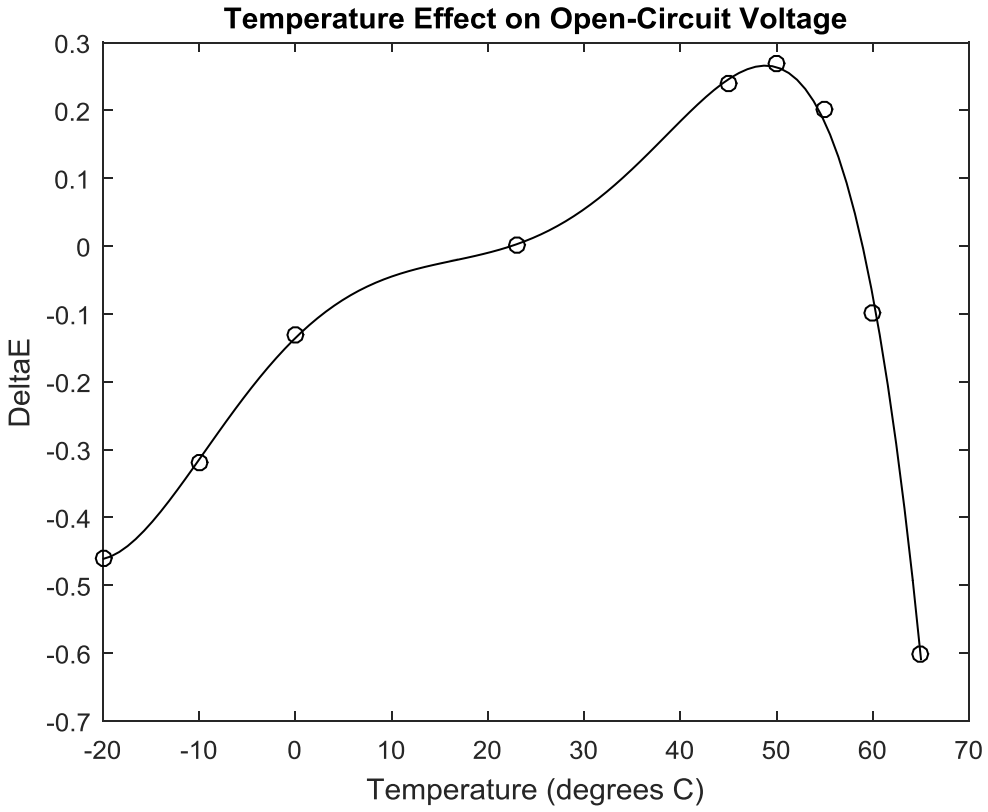

Figure 6

Specific Heat Capacity

The value used in the simulations is the measured specific heat of the Sony US-18650 lithium-ion battery: 1.04±0.02 J/g·K [6].

SECTION III

RESULTS

Every simulation produces a wealth of data. Extensive analysis of this data is beyond the scope of this paper (and hasn't been done yet), but here I will present some examples of the results available from the simulation.

Figure 7 shows the survival time of the UAV described in Section II.B, except that the payload and outside temperature have been varied.

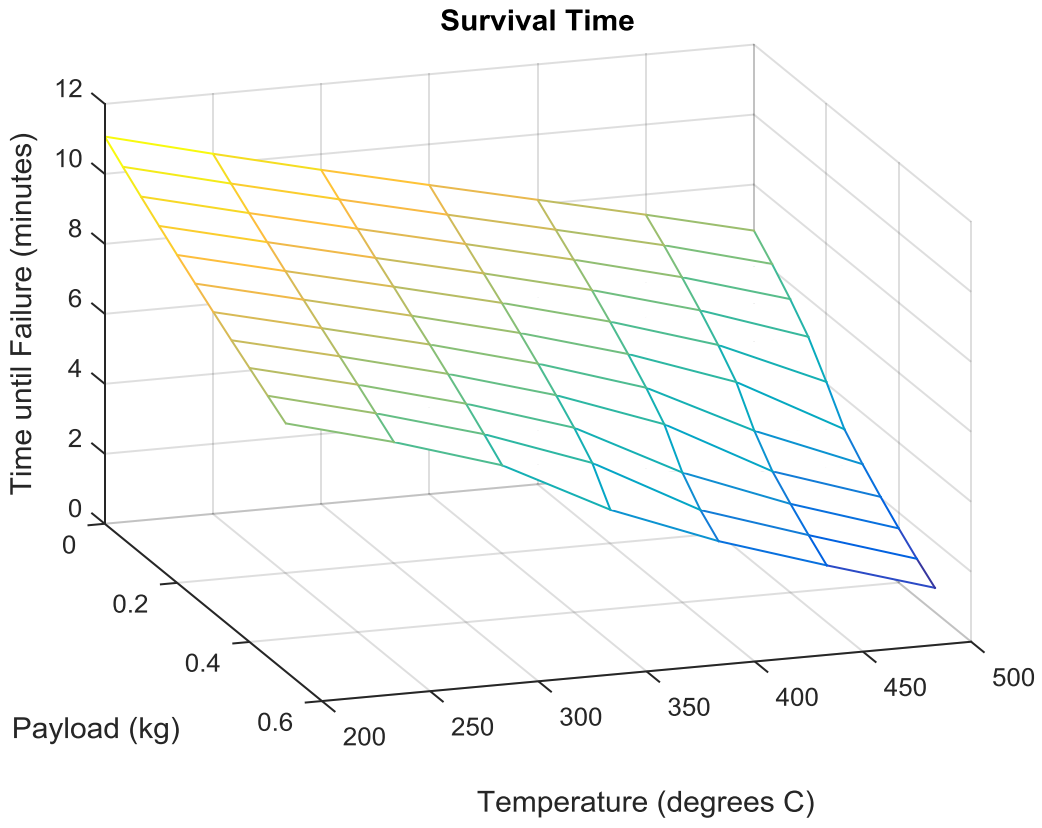

Figure 7

As would be expected, higher outside temperatures and heavier payloads reduce the time that the UAV can stay in the air. The most interesting insight from these simulations is that a consumer UAV, modified with only a few hundred grams of insulation and PCM and a different propeller, can survive for several minutes in extreme heat, and can even take off with an additional 500g payload in a 500°C environment!

I varied the payload and outside temperature, but any of the input variables listed in Section II.B could be varied to produce a similar graph. The results could be used to determine, for example, the ideal battery for a particular mission. Alternatively, one could use data on the internal state of the UAV to determine how to improve a design. For example, Figure 8 shows the temperature of the motors and battery on the UAV described in Section II.B.

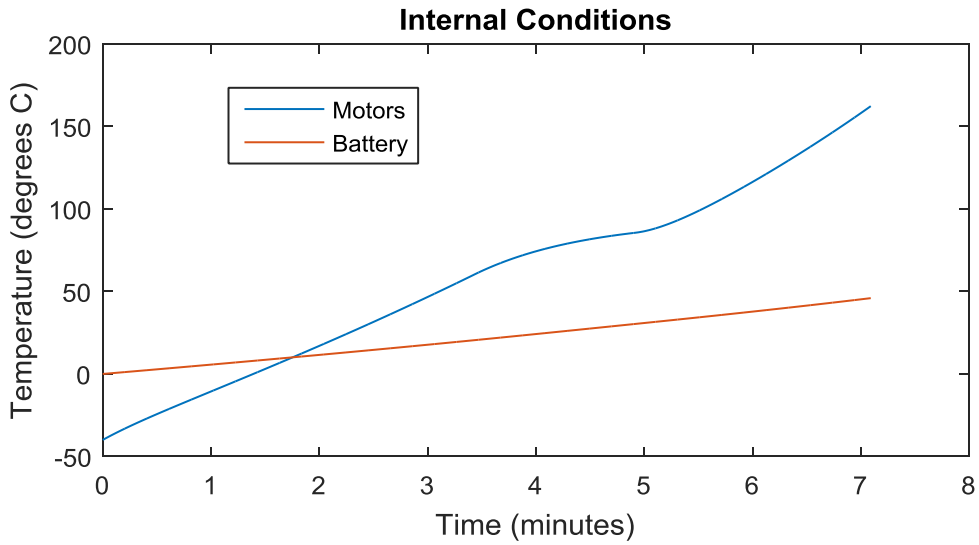

Figure 8

Here, it is readily apparent that the design would be best served by better protecting the motors. By the end of the flight, the motors are so hot that their efficiency has dropped to 60.7%, but the battery's PCM hasn't even started its phase change!

SECTION IV

CONCLUSION

The model succeeds in capturing the effects of extreme temperature on a UAV's performance. Its greatest omission is probably the electronic speed controllers (ESCs), which generate so much heat that they easily overheat. The greatest drawback is the difficulty in calculating certain parameters, such as the thermal resistances. Some parameters, such as the discharge curve, must be determined experimentally. On the other hand, the model can be applied to almost any UAV in almost any environment. Even different planets could be modelled by changing the right parameters.

Future research in this area could go in several directions. Future student researchers may perform experiments to test the accuracy of the model, or they may use the model to research the effect of different parameters on the survival time of a UAV or design a UAV for one specific mission—the results presented here only scratch the surface. Alternatively, they could take a different direction and use the model to simulate UAVs in extremely cold conditions.

REFERENCES

[1] J. B. Brandt, R. W. Deters, G. K. Ananda and M. S. Selig, "UIUC Propeller Data Site," University of Illinois at Urbana-Champaign, 2015. [Online]. Available: http://m-selig.ae.illinois.edu/props/propDB.html.

[2] D. Montone, "Temperature Effects on DC Motor Performance," Pittman Motors.

[3] L. Gao, L. Shengyi and R. A. Dougal, "Dynamic Lithium-Ion Battery Model for Simulation," *IEEE Transactions on Components and Packaging Technologies,* vol. 25, no. 3, pp. 495-505, 2002.

[4] DJI, "Matrice 100," 24 March 2016. [Online]. Available: https://dl.djicdn.com/downloads/dev/Matrice/en/M100_User_Manual_v1.6_en_160324.pdf.

[5] DJI, "E800 3510 Motor CCW," 2016. [Online]. Available: http://store.dji.com/product/e800-3510-motor-ccw.

[6] H. Maleki, S. Al Hallaj, J. R. Selman, R. B. Dinwiddie and H. Wang, "Thermal Properties of Lithium-Ion Battery and Components," *Journal of The Electrochemical Society,* vol. 146, no. 3, pp. 947-954, 1999.

[7] "PCM Summary," PCM Products Ltd., 2013. [Online]. Available: http://www.pcmproducts.net/files/PCM%20Summary%202013-S.pdf. [Accessed 17 March 2017].

[8] R. Gogoana, "Internal Resistance Variances in Lithium-Ion Batteries and Implications in Manufacturing," Massachusetts Institute of Technology, Cambridge, 2012.

APPENDIX 1

SIMULATION CODE

```
%% To run a single simulation, comment out this section and the last
% section. To run a series of simulations at different temperatures and
% masses, comment out the first two lines of the next section.
Mass = 0:0.05:0.5;
Temperature = 200:50:500;
I = length(Mass);
J = length(Temperature);
failuretime = zeros(I, J); % matrix of failure times (in seconds)
h = waitbar(0, ['Running simulation 1 of ' num2str(I*J) '.']);
sim = 0;
for i = 1:I
    m_payload = Mass(i);
    for j = 1:J
        T_inf = Temperature(j)+273.15;
        sim = sim + 1;
        waitbar(sim/I/J, h, ['Running simulation ' num2str(sim) ' of '
num2str(I*J) '.'])

        %% Mission parameters and initial conditions
%         m_payload = 0.3; % mass of payload in kg
%         T_inf = 300 +273.15; % outside temperature in K
        p = 101325; % air pressure in Pa
        T_m = -40 +273.15; % initial temperature of motor in K
        T_b = 0 +273.15; % initial temperature of battery in K
        SOD = 0; % battery's initial state of discharge (0 means fully
charged)
        m_PCM_m = 0.0106; % mass of PCM for each motor in kg
        m_PCM_b = 0.0676; % mass of PCM for battery in kg

        %% Physical constants
        g = 9.80665; % gravity in m/s^2
        R = 287.04; % gas constant for air in J/kg*K

        %% UAV configuration and properties
        m_other = 1.331; % mass of frame (without battery or motors) in kg

        % Propellers
        C_T = 0.0035; % torque constant
        C_F = 0.032; % thrust constant
        r = 0.173; % radius in m

        % Motor
        K_V_i = 30/pi/ 350; % voltage constant at 298.15K in V*s/rad
        alpha_mag = -0.0012; % temperature coefficient of motor magnet
(NdFeB) in K^-1
        n = 4; % number of motors
        m_m = 0.106; % mass of each motor in kg
        c_m = 386; % specific heat capacity of motor (copper) in J/kg*K
        R_m_i = 0.8182; % resistivity of copper at 293.15K in Ohm-m
```

```
        alpha_rho = 0.00386; % temperature coefficient of resistivity of
copper in K^-1
        M_frict = 0; % friction torque on each motor

        % Battery
        m_b = 0.676; % mass of battery in kg
        R_b = 0.168; % internal resistance of battery in Ohms
        C = 20520; % nominal battery capacity in C
        c_b = 1040; % specific heat of battery in J/kg*K
        % Polynomial coefficients for calculating battery potential
        c_k = [-21.811330223909493;21.828407952697490;-
9.565539058828605;24.719876447875457];
        c_E = [-8.477428441365285e-09;6.423656476635919e-07;-
3.151466598794766e-06;-5.069531428133001e-04;0.013901966075009;-
0.135627810858212];

        % Insulation
        m_ins_m = 0.0265; % mass of each motor's insulation in kg
        m_ins_b = 0.124; % mass of the battery's insulation in kg

        % Phase Change Material
        T_PCM = 46 +273.15; % temperature of phase change in K
        T_PCM_m = T_m; % PCM starts at the same temperature as whatever it's
surrounding.
        T_PCM_b = T_b;
        c_PCM = 2410; % specific heat capacity of PCM in J/kg*K
        L = 210000; % specific latent heat of PCM in J/kg

        % Thermal resistances in K/W
        R_T_m = 29.12467314;
        R_c_m = 1.278016947;
        R_T_PCM_m = 140.8006863;
        R_T_b = inf;
        R_c_b = 0.008066;
        R_T_PCM_b = 12.45653;

        %% Calculated constants
        % Latent heat capacity of PCM
        PCM_b = L*m_PCM_b;
        PCM_m = L*m_PCM_m;

        % Total mass of UAV in kg
        m = m_b + m_PCM_b + m_ins_b + n * (m_m + m_PCM_m + m_ins_m) + m_other
+ m_payload;

        % Angular velocity of propellers in rad/s
        Omega = sqrt(2*m*g*T_inf*R/n/p/pi/r^4/C_F);

        % Torque from air resistance on each propeller
        M_L = C_T * r / n / C_F * m * g;

        %% Initialize time and failure variables
        t = 0;
        dt = 0.25; % time step for simulation
        step = 0; % time step number
```

```
        failure = 0;

        %% Simulation
        while ~failure
            step = step + 1;
            t = step * dt;
            %% Temperature-dependent properties of motor
            K_V = K_V_i * (1 + alpha_mag * (T_m(step) - 298.15));
            R_m = R_m_i * (1 + alpha_rho * (T_m(step) - 293.15));

            I_m = (M_L + M_frict) / K_V; % current required by each motor in
A
            V_m = K_V * Omega + I_m * R_m; % potential required by the motors
in V

            %% Electrical properties of battery
            % Open-circuit battery potential in V
            V_b = polyval(c_k, SOD(step)) + polyval(c_E, T_b(step) - 273.15);

            % Current required from battery in A
            I_b = n * I_m;

            % Voltage available to the motors in V
            E_b = V_b - I_b * R_b;

            %% Heat transfer
            % Heat generated by each motor in W
            Q_m = I_m * V_m - Omega * M_L ;

            T_m(step+1) = T_m(step) + ((T_inf - T_m(step))/R_T_m +
(T_PCM_m(step) - T_m(step))/R_c_m + Q_m)/m_m/c_m*dt;
            T_PCM_m(step+1) = T_PCM_m(step) + ((T_inf -
T_PCM_m(step))/R_T_PCM_m + (T_m(step) -
T_PCM_m(step))/R_c_m)/m_PCM_m/c_PCM*dt;

            % Phase change
            if (T_PCM_m(step+1)>T_PCM)&&(PCM_m>0)
                PCM_m=PCM_m-(T_PCM_m(step+1)-T_PCM)*c_PCM*m_PCM_m;
                T_PCM_m(step+1)=T_PCM;
            end

            % heat generated by battery in W
            Q_b = I_b^2 * R_b;

            T_b(step+1) = T_b(step) + ((T_inf - T_b(step))/R_T_b +
(T_PCM_b(step) - T_b(step))/R_c_b + Q_b)/m_b/c_b*dt;
            T_PCM_b(step+1) = T_PCM_b(step) + ((T_inf -
T_PCM_b(step))/R_T_PCM_b + (T_b(step) -
T_PCM_b(step))/R_c_b)/m_PCM_b/c_PCM*dt;

            % Phase change
            if (T_PCM_b(step+1)>T_PCM)&&(PCM_b>0)
                PCM_b=PCM_b-(T_PCM_b(step+1)-T_PCM)*c_PCM*m_PCM_b;
                T_PCM_b(step+1)=T_PCM;
            end
```

```
            %% Discharge
            % Current-dependent discharge coefficient
            alpha = 1 + 0.092 / 2.52 * (5400 / C * I_b - 0.7);

            % Temperature-dependent discharge coefficient
            Beta = 1 - 0.111 / 65 * (T_b(step) - 296.15);

            SOD(step+1) = SOD(step) + alpha * Beta * I_b * dt / C;

            %% Failure condition
            if E_b < V_m
                failure = t;
            end
        end
%% Plot results
        failuretime(i, j) = failure;
    end
end
close(h)
Mass = repmat(Mass(:), 1, J);
Temperature = repmat(Temperature(:)', I, 1);
mesh(Mass, Temperature, failuretime/60)
xlabel('Payload (kg)')
zlabel('Time until Failure (minutes)')
ylabel('Temperature (degrees C)')
title('Survival Time')
```

APPENDIX 2

CALCULATION OF THERMAL RESISTANCES

To simplify calculation of thermal resistances, the battery and motor systems are modelled as concentric spheres, as shown in Figure 9.

The diameter of each of each component is calculated by setting the surface area of a sphere equal to the actual surface area of the component:

$$\pi d^2 = S \tag{38}$$

where d is the equivalent diameter and S is the surface areas of the component. The PCM is assumed to be a hollow sphere surrounding the component, so that its outer diameter is

$$d_{PCM} = \left(d^3 + \frac{6m_{PCM}}{\pi\rho_{PCM}}\right)^{\frac{1}{3}} \tag{39}$$

where ρ_{PCM} is the density of the PCM.

The PCM is assumed to be surrounded by a hollow sphere of insulation. By making the inner diameter of the insulation larger than the outer diameter of the PCM, a layer of air (or, potentially, a vacuum) becomes another effective layer of insulation without adding weight. If the inner diameter of the insulation (the outer diameter of the air) is d_{air}, then the mass of the insulation is

$$m_{ins} = \rho_{ins}\frac{\pi}{6}(d_{ins}^3 - d_{air}^3) \tag{40}$$

The battery and its PCM are assumed to be suspended inside the insulation by tiny wires with negligible contribution to heat transfer. The motor, on the other hand, must be secured by a strong motor mount, and also must have a metal shaft connecting it to the propeller. The mount and shaft are easy paths for heat to enter the motor.

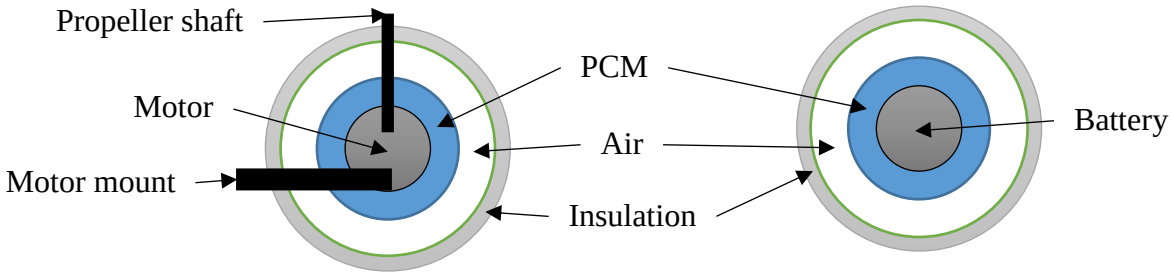

Figure 9

The thermal resistance through any one of these layers is

$$R = \frac{1}{kS} \tag{41}$$

where k is the material's thermal conductivity and S is a shape factor. For hollow spheres, the shape factor is

$$S = \frac{2\pi d_i d_o}{d_o - d_i} \tag{42}$$

where d_i and d_o are the inner and outer diameters, respectively; for prisms (the motor mount and propeller shaft) the shape factor is simply

$$S = \frac{A}{l} \tag{43}$$

where A is the cross-sectional area and l is the length from the environment to the motor.

Thermal resistances are mathematically similar to electrical resistances, with temperature differences being analogous to voltage and heat transfer being analogous to current. Figure X shows the thermal circuits that were used to calculate the thermal resistances used in the model's heat transfer equations.

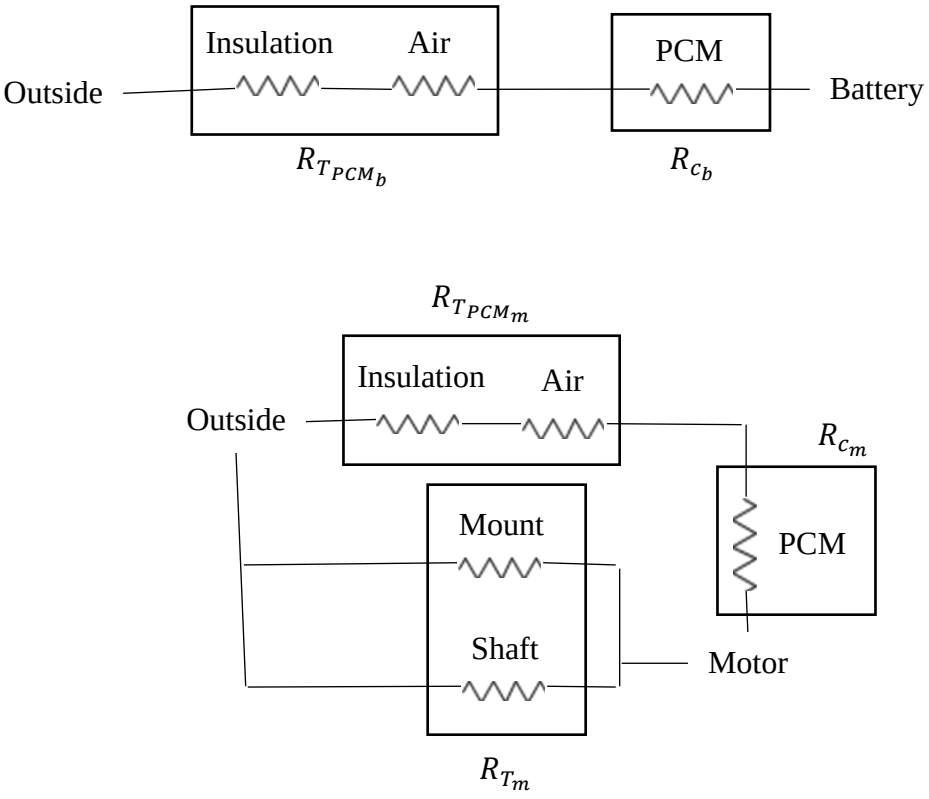

Figure 10

With these equations and models, one needs the surface area of each component; the mass and density of the PCM; the thicknesses of insulation and air; the dimensions of the motor mount and propeller shaft; and the thermal conductivities of the PCM, insulation, and, shaft, and mount to determine all six thermal resistances.

The DJI 3510 motors are roughly cylindrical, with a diameter of 35mm and a height of 10mm; as per Equation (38), their equivalent diameter is 31.0mm. The TB48D battery is essentially an 89mm×132mm×191mm rectangular prism, so its equivalent diameter is 185mm.

Table 7 summarizes the parameters of the motor system.

Table 7

Parameter	**Symbol**	**Value**	**Comments**
Equivalent diameter of motor	d_m	31.0mm	
Mass of PCM	m_{PCM_m}	10.6g	
Density of PCM	ρ_{PCM}	1587 kg/m^3	PCM S46
Thickness of air	t_{air}	45mm	
Thickness of insulation	t_{ins}	5mm	
Length of mount and shaft	L	52.0mm	$\frac{1}{2}(d_{ins} - d_m)$
Area of mount	A_{mount}	1 cm^2	
Area of shaft	A_{shaft}	12.6 mm^2	Cylinder with radius of 2mm
Thermal conductivity of PCM	k_{PCM}	450 mW/m·K	PCM S46
Thermal conductivity of air	k_{air}	24 mW/m·K	
Thermal conductivity of insulation	k_{ins}	24 mW/m·K	Silica aerogel
Thermal conductivity of mount	k_{mount}	15.2 W/m·K	Silicon carbide
Thermal conductivity of shaft	k_{shaft}	21.0 W/m·K	Titanium

Table 8 summarizes the parameters of the battery system.

Table 8

Parameter	**Symbol**	**Value**	**Comments**
Equivalent diameter of battery	d_b	185mm	
Mass of PCM	m_{PCM_b}	67.6g	
Density of PCM	ρ_{PCM}	1587 kg/m^3	PCM S46
Thickness of air	t_{air}	45mm	
Thickness of insulation	t_{ins}	5mm	
Thermal conductivity of PCM	k_{PCM}	450 mW/m·K	PCM S46
Thermal conductivity of air	k_{air}	24 mW/m·K	
Thermal conductivity of insulation	k_{ins}	24 mW/m·K	Silica aerogel

The insulation is kept thin to reduce weight; because air has approximately the same thermal conductivity as the insulation, the insulation is only required as a physical barrier between the internal and external air. The density of silica aerogel is 100 kg/m^3, so, from Equation (40), we can find that the mass of the insulation surrounding each motor is 26.5g and the mass of the insulation surrounding the battery is 124g.

The thermal resistances obtained from all these calculations are summarized in Table 9.

Table 9

R_{c_m}	R_{T_m}	$R_{T_{PCM_m}}$	R_{c_b}	R_{T_b}	$R_{T_{PCM_b}}$
1.28 K/W	29.1 K/W	141K/W	0.00807 K/W	∞	12.5 K/W

APPENDIX 3

ANALYTICAL SOLUTIONS TO LINEARIZED HEAT TRANSFER EQUATIONS

Heat Transfer Before and After Phase Change

The following thermal analysis is carried out with the assumption that the heat generated by the motor and by the battery is constant, thus linearizing the previously introduced nonlinear system. The governing equations for the motor system and the battery system are identical; therefore, the following derivation can be applied to either system.

Heat flow between the component, the phase-change material, and the ambient environment was described in Section II.A.4. Equation (27) for the motor or (31) for the battery can be rewritten as Equation (44); and Equation (34) or (35) can be rewritten as Equation (45).

$$\frac{1}{R_T}(T - T_\infty) + \frac{1}{R_c}(T - T_{PCM}) - \dot{Q}_{waste} = -mc\frac{dT}{dt} \tag{44}$$

$$\frac{1}{R_{T_{PCM}}}(T_{PCM} - T_\infty) + \frac{1}{R_c}(T_{PCM} - T) = -m_{PCM}c_{PCM}\frac{dT_{PCM}}{dt} \tag{45}$$

where $\dot{Q}_{waste}$ is the waste heat generated by the component. These equations can be rearranged to arrive at Equations (46) and (47).

$$T(D + K_1 + K_2) - K_1 T_\infty - K_2 T_{PCM} - K_5 = 0 \tag{46}$$

$$T_{PCM}(D + K_3 + K_4) - K_3 T_\infty - K_4 T = 0 \tag{47}$$

Here D represents a first order differential operator with respect to time and K_i are constants used to simplify the differential equations. The value of these constants are expressed in Equations (48) through (51).

$$K_1 = \frac{1}{R_T mc} \tag{48}$$

$$K_2 = \frac{1}{R_c mc} \tag{49}$$

$$K_3 = \frac{1}{R_{T_{PCM}} m_{PCM} c_{PCM}} \tag{50}$$

$$K_4 = \frac{1}{R_c m_{PCM} c_{PCM}} \tag{51}$$

$$K_5 = \frac{\dot{Q}_{waste}}{mc} \tag{52}$$

Equations (46) and (47) can then be solved simultaneously, leading to a single second order differential equation for the temperature of the phase-change material as a function of time.

$$\begin{aligned} D^2\left(\frac{T_{PCM}}{K_4}\right) + D\left(T_{PCM} + \frac{K_1 T_{PCM}}{K_4} + \frac{K_2 T_{PCM}}{K_4} + \frac{K_3 T_{PCM}}{K_4}\right) \\ + \left(\frac{K_1 K_3 T_{PCM}}{K_4} + \frac{K_2 K_3 T_{PCM}}{K_4} + K_1 T_{PCM}\right) \\ = \left(K_5 + K_1 T_\infty + \frac{K_1 K_3 T_\infty}{K_4} + \frac{K_2 K_3 T_\infty}{K_4}\right) \end{aligned} \tag{53}$$

Equation (53) can then be rearranged to form Equation (54).

$$T_{PCM}\left(D^2 + D(K_1 + K_2 + K_3 + K_4) + (K_1K_3 + K_2K_3 + K_1K_4)\right) = K_5K_4 + (K_1K_4 + K_1K_3 + K_2K_3)T_\infty \quad (54)$$

The solution of this differential equation takes the form shown in Equation (55).

$$T_{PCM}(t) = \mathrm{C}_0 + C_1 \exp(\gamma_1 t) + C_2 \exp(\gamma_2 t) \quad (55)$$

Here C_0 is the particular solution and C_1 and C_2 are constants. The particular solution can be determined by substituting it into Equation (54) as the temperature of the phase-change material.

$$C_0(K_1K_3 + K_2K_3 + K_1K_4) = K_5K_4 + (K_1K_3 + K_2K_3 + K_1K_4)T_\infty \quad (56)$$

Therefore the particular solution is given by Equation (57).

$$C_0 = \frac{K_5K_4}{K_1K_3 + K_2K_3 + K_1K_4} + T_\infty \quad (57)$$

The solution for the temperature of the phase-change material can then be substituted into Equation (44) or (45) to obtain the temperature of the component as a function of time. The solution for the temperature of the phase change material is shown in Equation (58).

$$T_{PCM}(t) = \frac{K_5K_4}{K_1K_3 + K_2K_3 + K_1K_4} + T_\infty + C_1 \exp(\gamma_1 t) + C_2 \exp(\gamma_2 t) \quad (58)$$

The time constants are the solutions to Equation (59), the characteristic equation:

$$\gamma^2 + (K_1 + K_2 + K_3 + K_4)\gamma + K_1K_3 + K_2K_3 + K_1K_4 = 0 \quad (59)$$

Because the thermal resistances are all positive, the time constants must be negative.

The solution for the temperature of the component is given by Equation (60).

$$T(t) = \frac{K_5(K_3 + K_4)}{K_1K_3 + K_2K_3 + K_1K_4} + T_\infty + C_1\frac{\gamma_1 + K_3 + K_4}{K_4}\exp(\gamma_1 t) + C_2\frac{\gamma_2 + K_3 + K_4}{K_4}\exp(\gamma_2 t) \quad (60)$$

The constants C_1 and C_2 can be found by substituting the initial component and phase-change material temperatures into the solutions. After phase transformation, the initial temperature of the phase change material is taken to be the melting temperature of the PCM, and the initial temperature of the component is taken to be the temperature at the end of the PCM phase change.

Using T_i and T_{PCM_i} to be the initial temperatures of the component and PCM, respectively, the constants are

$$C_1 = \frac{(\gamma_2 + K_3)T_\infty + K_4T_i - (\gamma_2 + K_3 + K_4)T_{PCM_i}}{\gamma_1 - \gamma_2} + \frac{\gamma_2}{\gamma_1 - \gamma_2}\frac{K_5K_4}{K_1K_3 + K_2K_3 + K_1K_4} \quad (61)$$

$$C_2 = \frac{(\gamma_1 + K_3)T_\infty + K_4T_i - (\gamma_1 + K_3 + K_4)T_{PCM_i}}{\gamma_2 - \gamma_1} + \frac{\gamma_1}{\gamma_2 - \gamma_1}\frac{K_5K_4}{K_1K_3 + K_2K_3 + K_1K_4} \quad (62)$$

Heat Transfer During Phase Change

The following thermal analysis is carried out with the assumption that the heat generated by the component and the temperature of the phase-change material are constant.

While the phase change material undergoes phase transformation, the heat flow away from the component is given by Equation (63).

$$T(D + K_1 + K_2) - T_\infty K_1 - T_{trans} K_2 - K_5 = 0 \tag{63}$$

The heat flow away from the phase change material is the same as previously shown in Equation (45). The differential equation representing the component temperature and time is given by Equation (64).

$$\frac{dT}{dt} + (K_1 + K_2)T = T_\infty K_1 + T_{trans} K_2 + K_5 \tag{64}$$

To solve the differential equation, Equation (64) can be multiplied by an integration factor, given in Equation (65).

$$u(t) = \exp\big((K_1 + K_2)t\big) \tag{65}$$

This produces Equation (66).

$$\begin{aligned} \exp\big((K_1 + K_2)t\big)\frac{dT}{dt} + \exp\big((K_1 + K_2)t\big)(K_1 + K_2)T \\ = \exp\big((K_1 + K_2)t\big)(TK_1 + T_{trans}K_2 + K_5) \end{aligned} \tag{66}$$

Rearranging, this equation produces Equation (67).

$$\frac{d}{dt}\big(\exp\big((K_1 + K_2)t\big)T\big) = \exp\big((K_1 + K_2)t\big)(T_\infty K_1 + T_{trans}K_2 + K_5) \tag{67}$$

Integrating both sides generates the solution to the equation, given by Equation (68).

$$\exp\big((K_1 + K_2)t\big)T = \frac{T_\infty K_1 + T_{trans}K_2 + K_5}{K_1 + K_2}\exp\big((K_1 + K_2)t\big) + C \tag{68}$$

Where C is a constant of integration. The solution can then be rearranged to solve for the component temperature during PCM phase change as a function of time. It should be noted that the temperature of the phase-change material remains constant during this time.

$$T(t) = \frac{T_\infty K_1 + T_{trans} K_2 + K_5}{K_1 + K_2} + C \exp(-(K_1 + K_2)t) \tag{69}$$

The integration constant, C, can then be solved for by inputting the initial component temperature: the temperature of the component at the onset of PCM phase transformation.

$$C = T_i - \frac{T_\infty K_1 + T_{trans} K_2 + K_5}{K_1 + K_2} \tag{70}$$